RSC Advances

ROYAL SOCIETY OF CHEMISTRY

www.rsc.org/advances

Journal Name

COMMUNICATION

Sustainable conversion of cellulosic biomass to chemicals under visible-light irradiation

Lina Wang,[a] Zhanying Zhang,[b] Lixiong Zhang,[c] Song Xue,[d] William O. S. Doherty,[b] Ian M. O'Hara [b] and Xuebin Ke*[a]
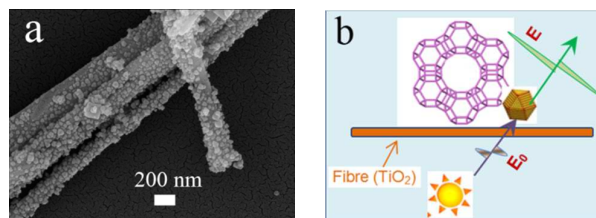
For the first time, the conversion of crystalline cellulose to valuable chemicals was enhanced by visible-light irradiation using zeolite-based gold nanoparticles (Au-NPs). This plasmon-enhanced photocatalytic conversion significantly improved processing efficiency and achieved a high yield of 60% at relative low temperature. Moreover, the photocatalytic properties of the photocatalysts varied directly with the light intensity and the irradiation wavelength.

With diminishing fossil resources and increasing concerns about environmental issues, biomass conversion becomes attractive for the production of fuels and chemicals.[1,2] Cellulose, the most abundant non-food biomass on earth, is a promising renewable feedstock. It is estimated that the world-wide production of cellulose amounts to 110 billion tons/year.[3,4]

Cellulose is a water insoluble saccharide polymer composed of glucose monomers linked by β-1,4 glycosidic bonds. Apart from enzymatic hydrolysis, acid catalysis is another promising option for cellulose conversions, which initially produce chemical intermediates or valuable chemicals and subsequently proceed to biofuels. Mineral acids including H_2SO_4, HCl and HBr, have demonstrated a high efficiency toward the hydrolysis of cellulose, up to 80% of yield.[5,6] Generally, homogeneous catalysts can exhibit higher yields at relative mild conditions. However, the catalysts themselves are subject to environmental concerns (corrosion and pollution) in product separation and device maintenance.

The attention is turning to the solid acid catalysts in companying with ever-increasing demands for energy and environment.[7,8] Solid acid catalysts, such as metal oxides,[9,10] metal phosphate,[11,12] polymer based acid resins,[13,14] sulphonated carbonaceous acids,[15,16] heteropoly acids,[17-19] H-form zeolites,[20] normally carry a high concentration of strong Brønsted acid sites embedded into an acidic environment. Moreover, these solid acid catalysts possess a high affinity to poly-saccharides structure, suitable for cellulose hydrolysis.[21]

Great progresses on solid acid catalysis have been made in biomass conversion to produce chemicals or fuels in terms of catalyst structures, active sites, reaction media, and pre-treatment technologies. However, the mass diffusion between crystalline cellulose and solid catalysts seriously impedes practical productions of chemicals from cellulose. Without the assistance of milled or microwaved treatment, the yields are often below 50% and get primary products of glucose and reducing sugars of wide distributions. With more easily degraded feedstock, such as amorphous cellulose, cellobiose, glucose and fructose, the conversion can be conducted at a mild condition (<120 ^{o}C).[3,4] Current processes for cellulose conversion (including pyrolysis) always require high temperatures (>200 °C) and/or high pressures (>20 bar), which are suffering from low product selectivity, high energy consumption and catalyst instability. Thus, it is imperative to develop energy-efficient processes for cellulose conversion.

[a.] School of Chemistry, Physics and Mechanic Engineering, Queensland University of Technology. Brisbane, QLD 4101, Australia. Fax: +61 731381804; Tel:+ 61 731389197; E-mail: x.ke@qut.edu.au

[b.] Centre for Tropical Crops and Biocommodities, Queensland University of Technology, Brisbane, QLD 4001, Australia.

[c.] State Key Laboratory of Materials-Oriented Chemical Engineering, College of Chemistry and Chemical Engineering, Nanjing University of Technology, Nanjing 210009, China.

[d.] School of Chemistry & Chemical Engineering, Tianjin University of Technology, Tianjin 300384, China.

† Electronic Supplementary Information (ESI) available: Experimental details, product distributions for cellulose conversion varying with light intensity, mechanism of converting glucose to HMF. See DOI: 10.1039/x0xx00000x

Scheme 1. Advanced nanostructure for cellulose conversion: a) Zeolites on nanofibres (zeolite#NFs); b) Metals coated zeolite#NFs with oriented open pores and enhanced electromagnetic fields, $E/E_0=10^3$-10^6 times.

In this communication, for the first time photocatalytic conversions were proposed to enhance cellulose hydrolysis utilising a new plasmonic nanostructure, which was composed of TiO_2 nanofibres (NFs) supported H-form Y-zeolites (HY) decorated with Au-NPs (Au-HYT). Firstly, highly efficient nanocatalysts were designed to enhance the mass transfer (Scheme 1). Nanozeolites (< 100 nm) were grown on ultrathin nanofibres, where the open pores of the nanozeolites were controlled, to expose active sites and porous channels. This design facilitated the dissolved/degraded reactants access to active sites inside channels, therefore benefiting catalyst selectivity.[22,23] More importantly, the new nanocatalysts could be decorated with plasmonic metals, such as Au-NPs, which functioned as "antennas" to efficiently absorb visible light. The localised surface plasmon resonance (LSPR) effect is a physical absorption of light, which produces an enhancement of electromagnetic field up to 10^3-10^6 folds locally. Plasmonic metals have recently been explored for efficient photochemical synthesis.[24,25] We have found that Au-NPs can significantly enhance zeolite photocatalysis with high product selectivity.[26,27]

This research aims to develop new catalysts materials and innovative process. The plasmonic structure of Au-HYT was originally explored and firstly used for cellulose conversion under light irradiation. Various solid acid catalysts, such as Au-NPs decorated zeolite Y on TiO_2 NFs (Au-YT), TiO_2 supported HY zeolites (HYT), TiO_2 supported Y zeolites (YT), HY zeolites and acid treatment TiO_2 NFs (HT), were also compared.
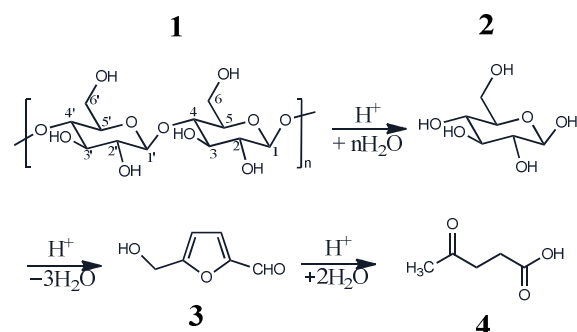
Scheme 2. Catalytic procedures of cellulose conversion. **1**. Cellulose; **2**. Glucose; **3**. 5-hydrooxymethylfurfural (HMF); **4**. Levulinic acid (LeA).

The pre-treatment of feedstock, reactive media, and reaction conditions were decided according to relative documents.[3,4] The experimental procedure was detailed in supplementary information (SI). Generally, crystalline cellulose was firstly dissolved in 1-ethyl-3-methylimidazolium chloride (EMIMCl) solution. Subsequently, cellulose hydrolysis was initiated with addition of water and catalysts as well as light irradiation. If only with water as solvent, no products were detected. The water amount had a profound effect on cellulose solubility and swelling.[28] The 10% concentration of water in ionic liquids was selected, which assisted hydrolysis of cellulose as well as maintained cellulose swelling and solubility

to some extent. Generally, the conversion of cellulose went through several key stages (Scheme 2). When H^+ ions of solid acids attached to the β-1,4-glycosidic bonds, it caused a split in the cellulose chain to from glucose. Subsequently the dehydration of glucose produced 5-hydrooxymethylfurfural (HMF). Furthermore, the hydrolysis of HMF may produce Levulinic acid (LeA) or Humins.[5-8]

The acid strength of the catalyst was an important factor in activating crystalline cellulose towards hydrolysis. However, the network structure of cellulose endowed it with high chemical stability, thus processing must be performed under harsh conditions of high temperature and/or digestion by strong liquid acids. Under these reaction conditions, control of product selectivity was impossible due to the thermal instabilities of cellulose derived sugars. Many side-products were commonly fabricated, including the important "platform molecule" 5-hydroxymethylfurfural (HMF), LeA and humins.[3-8] In this work, the reaction yield indicated the production of valuable chemicals (glucose and HMF).

Table 1. The yield (%) of cellulose conversion with various catalysts

Catalysts[a]	Light on			Light-off		
	glucose	HMF	Total	glucose	HMF	Total
Au-HYT	48.1	10.6	58.7	15.5	0	15.5
Au-YT	30.2	2.6	32.8	10.2	0	10.2
HYT	14	10.1	24.1	11.1	7.5	18.6
YT	24.9	5.7	30.6	19.6	4.6	24.2
HY	20.2	19.1	39.3	18.9	17.1	36
HT	14.9	5.7	20.6	10.6	4.9	15.5

[a] Reaction conditions: 50 mg cellulose, 50 mg catalyst, 500 mg water, 4.5 g EMIMCl, 0.5 W cm-2 visible light, at 140 °C for 16 hours.

Plasmonic metal nanoparticles were loaded onto the solid acid catalysts to absorb visible light to enhance catalyst activity and product selectivity. This is feasible because light irradiation can intensify the strongly polarised electrostatic fields of zeolite extra-framework ions.[26,27] Table 1 showed the results of cellulose conversion with various catalysts, including Au-HYT, Au-YT, HYT, YT, HY and HT. The conversion of cellulose proceeded effectively on these catalysts even at mild reactive conditions. The catalytic conversions improved significantly on Au-HYT under visible light irradiation; particularly, the yields of glucose and HMF increased from 15.5% to 58.7% on Au-HYT. However, with light off Au-NPs have not such an effect and even impeded the conversion to HMF. This could be concluded by the comparison of Au-HYT and HYT. The similar situation happened on Au-YT and YT. These results indicated that Au-NPs themselves were not active sites under dark conditions and confirmed that visible light and Au-NPs were necessities to sharply boost cellulose conversion.

Moreover, the products mainly consisted of glucose and HMF, and no LeA produced under light irradiation on Au-HYT. It can be concluded that both LSPR effect and acid strength of new catalysts played important roles in the serial process for

cellulose conversion. The TiO$_2$ nanofibres had large external surface areas (~50 m^2 g^{-1}) and large aspect ratios (200 nm in diameter and 10 μm in length), which were easily to form networking structures and facilitated the dispersion and recycling of catalysts from liquid solution. Many efforts were made to reveal possible function mechanisms on cellulose conversion using the optimal catalysts of Au-HYT.
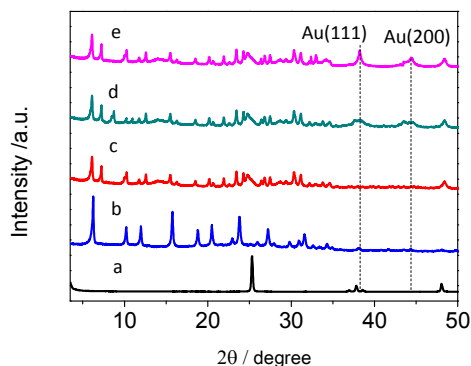

Figure 1. XRD patterns of various catalysts: a) HT; b) HY; c) YT/HYT; d) Au-YT; e) Au-HYT.

The crystal structures of various catalysts were detected by X-ray diffraction (XRD) patterns (Fig. 1), confirming that the zeolite structure preserved well after loads of Au-NPs. The characteristic peaks of zeolite Y at 2θ of 6.3°, 15.9° and 24.0° were reflections from the (111), (133) and (266) planes of zeolite Y, respectively. It indicated that the zeolite nano-crystals on the nanofibres were well crystallized.[22,23] A couple of new peaks (Fig. 1) around 38.2° and 44.5° were observed and assigned to the characteristic diffraction peaks of Au-NPs, corresponding to the Au (111) and (200) planes, respectively.[26,27]
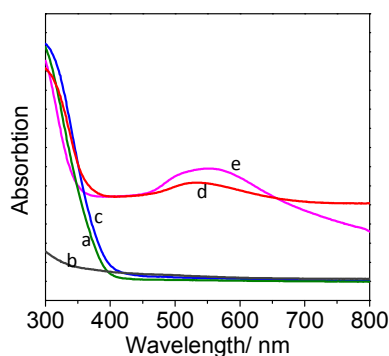

Figure 2. UV/Vis spectra of of various catalysts: a) HT; b) HY; c) YT/HYT; d) Au-YT; e) Au-HYT.

As shown in Figure 2, both TiO$_2$ NFs and Y-zeolites with or without acid treatment (H$^+$ exchange) did not have obvious absorption in the wavelength range of visible light region,

while catalysts of Au-NPs loads had strong absorption around 530 nm in the visible-light region. This LSPR effect can be harnessed in new catalyst systems therefore enhanced the catalytic conversion of cellulosic biomass. The loads of Au-NPs were about 3% in weight and the atom ratio of Si/Al was around 4.5 detected by the SEM-EDS, confirming the formation of zeolite Y in consistent with the XRD analysis. The TEM image indicated that the size of Au-NPs was around 5 nm (not shown).

Figure 3 showed the yield of valuable chemicals for cellulose conversion. The products mainly consisted of glucose and HMF under light irradiation and the produced LeA could be neglected. It indicated that the yields of valuable chemicals increase with higher temperature. The yield of glucose and HMF achieved 58.7% at 16 hours at 140 °C (Fig. 3a). After reaction time of 16 hours, the yields at 120 °C and at 130 °C continued to increase. In contrast, the reaction at 140 °C displayed a decline tendency after 16 hours (Fig. 3b-3d). The maximum yield of glucose and HMF at 16 hours at 140 °C can be attributed to the further conversions of HMF to generate solid humins, which are main side-products under light irradiation.[29,30] The yield at the same reaction condition but with light off was 3.5% at 140 °C for 24 hours.
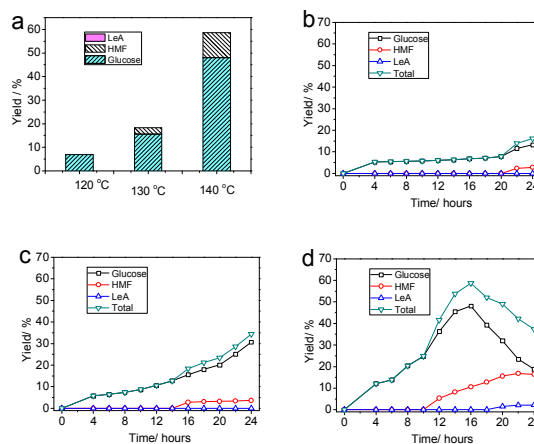

Figure 3. The yield for cellulose conversion on Au-HYT. a) The yields of valuable chemicals at different temperatures at 16 hours; b) The product distributions at 120 °C; c) The product distributions at 130 °C; d) The product distributions at 140 °C. Reaction conditions: 50 mg cellulose, 50 mg catalyst, 500 mg water, 4.5 g EMIMCl, 0.5 W cm^{-2} visible light, 24 hours.

One may argue that the acidity of zeolites plays a more important role than LSPR effect in the cellulose conversion because Brønsted acid sites (H$^+$) are the catalytic sites. However, this study conveyed a clear message that the polarised electromagnetic field due to LSPR effect of Au-NPs did contribute to improving the catalytic performances of zeolites under visible light irradiation. To illuminate the impacts of light irradiation on the cellulose conversions, the light intensity and the range of wavelength were investigated on Au-HYT at 130 °C with light on.
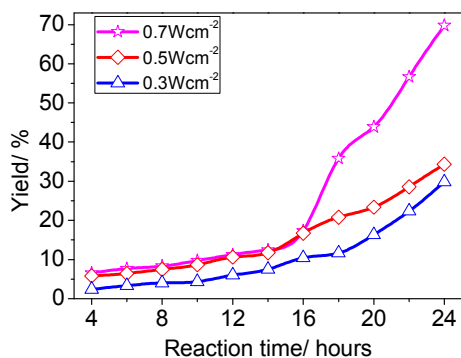
Figure 4. The yields of valuable chemicals for cellulose conversion varying with light intensity. Reaction conditions: 50 mg cellulose, 50 mg catalyst, 500 mg water, 4.5 g EMIMCl, at 130 °C for 24 hours.

Figure 4 illustrated the yields of valuable chemicals for cellulose conversion varying with light intensity. Hydrolysis of cellulose to glucose and subsequent formation of HMF were observed under light irradiation with different light intensities. The yield of LeA could be neglected, which was detailed in supplementary information (SI, Section 1). The yield of glucose and HMF at light intensity of 0.7 W cm^{-2} demonstrated the highest efficiency; achieving a total yield of 69.8% at 130 °C for 24 hours. The reaction rate at lower light intensity, such as at 0.5 W cm^{-2} and 0.3 W cm^{-2}, showed relative low conversions of 34.4% and 29.8%, respectively. It indicated that the conversion of cellulose can be activated or driven by a plasmonic nanostructure. Higher light intensity meant that more photons or more energy input originated from incident light at a certain excitation wavelength, which may efficiently interact with Au-NPs in the catalysts. This result indicated that increasing light intensity could enhance the LSPR effect on Au-HYT thus contributing to boosting the catalytic activity.
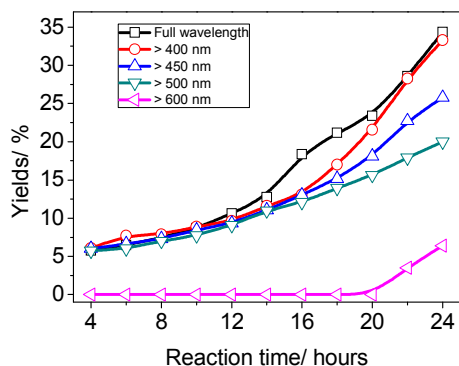

Figure 5. The yields of valuable chemicals for cellulose conversion varying with wavelength ranges. Reaction conditions: 50 mg cellulose, 50 mg catalyst, 500 mg water, 4.5 g EMIMCl, 0.5 W cm^{-2} visible light, at 130 °C for 24 hours.

The light wavelength was also investigated using glass filters to block photons with wavelengths below the filter threshold (see SI, Section 3). For example, the cut-off wavelength of 400 nm means that a majority of the light with wavelength smaller than 400 nm was blocked. Figure 5 showed that the light wavelength significantly influenced the catalytic activity of Au-HYT. The yield decreased remarkably, dropping from 34.4% to 6.4% while the wavelength ranges were narrowed from full wavelength to the wavelength large than 600 nm. The low yield of the latter was corresponding to the low light absorption of Au-NPs in this light ranges (the curve e in Figure 2). This result demonstrated a wavelength-selective enhancement on Au-HYT, and proved that visible light with wavelength around 530 nm could induce the LSPR effect of Au-NPs and made a primary contribution to boost the catalytic activity.
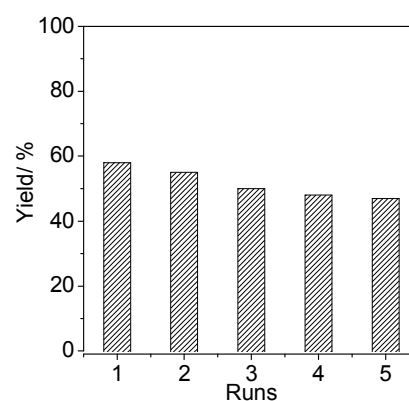

Figure 6. The yields of valuable chemicals for cellulose conversion with recycled catalysts. Reaction conditions: 50 mg cellulose, 50 mg catalyst, 500 mg water, 4.5 g EMIMCl, 0.5 W cm^{-2} visible light, at 140 °C for 16 hours.

Figure 6 showed the conversions of cellulose on Au-HYT recycled for four times. As far as we can see, the efficiency was reducing gradually from a yield around 60% to about 50% after 5-run use. The catalysts can maintain about 80% of the initial reactive activity after 5 runs. It indicated that the catalyst was very stable and the supported Au-NPs could be reused without leaching.[26,27] From the TEM image (see SI, Fig. S4), the 5 nm of Au-NPs, 100 nm of zeolites, and fibrous TiO_2 can be cleanly seen without obvious aggregations or amorphology. In thought that the recycling of catalysts was only conducted with drying procedure, the treatment of recycled catalysts, such as the removal of deposited carbon by calcination, should further improve the activity of recycled catalysts.

A mechanism for the hydrolysis of cellulose to glucose was outlined in Scheme 3. Basically solid acids (proton H^+) originated from zeolites or TiO_2 NFs, played a key role in hydrolysis of cellulose. Particularly, the LSPR effect of Au-NPs under visible light irradiation enhanced the polarity electrical field of the extra-framework cations in zeolites.[26,27] The polarity electrical field benefited to acid strength as well as stretched polarized bonds while attacked by proton H^+ (step I).

COMMUNICATION

The stretching further enhanced the negative character of the oxygen atom in the β-1, 4 glycosidic bond. Consistent with thermal reactions, the $C_{1'}$-O bond in the β-1, 4 glycosidic linkage was stretched and broke down to glucose and a positive carbon cation (step II). With polarized water molecular, the hydrolysis reaction at the positive carbon cation easily proceeded to produce glucose and release a proton H^+ (step III).[31]
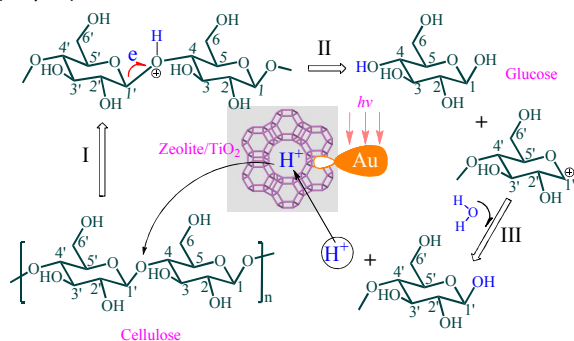
Scheme 3. The processing mechanism for the hydrolysis of cellulose to glucose under light irradiation on Au-HYT.

Similarly, the subsequent conversion from glucose to HMF went through a dehydration process assisted by solid acid catalysts (see SI, Scheme S1). Apart from the solid acid (proton H^+) attacking the O in C-O-C (step I in SI, Scheme S1), the glucose underwent an opening-cycle reaction. Meanwhile, a carbonyl bond is formed (step II in SI, Scheme S1), which could be enhanced by plasmonic structure (Au-NPs) and had been well documented by our previous works as well as other groups. To make it simple, this process to form a carbonyl bond is similar to the oxidation of alcohols, where the electromagnetic fields enhanced by LSPR effect of Au-NPs produced energetic electrons and thus promote the hydrogen-abstracting process.[26,27,32-34] Subsequently, the continuous inter-molecular dehydration processes proceeded. After losing 3 water molecules in total (steps II-IV in SI, Scheme S1), the HMF could be formed. During this process, both acid strength and LSPR effect played crucial roles. The effect of light irradiation on ionic liquids will be further investigated apart from function as solvents.

Conclusions

The communication unravels a plasmonic enhancement effect under visible light irradiation for the conversion of cellulosic biomass. The new plasmonic nanostructure can efficiently absorb visible light by means of supported Au-NPs on active zeolite catalysts. Moreover, light energy interacts directly with active sites of catalysts and avoids the heating of the whole solvent system. Therefore reactions can be conducted at moderate conditions. This study demonstrated the influences of reaction temperatures, light intensity and light wavelength for cellulose conversion to valuable chemicals. Under mild conditions, the yield of glucose and HMF achieved above 60%

at 130 °C for 24 h. Both the acid strength and LSPR effect of Au-NPs have key impacts on processing efficiency. The processing mechanism was proposed with the acid strength enhanced by the polarized electrical fields of zeolites due to the LSPR effect. The outcomes would significantly decrease processing costs, reduce energy consumption, and contribute to the utilisation of broad biomass resources. This research has great potential to make biofuel and chemical productions renewable. More significantly, due to the solid nature of the catalysts, the separation and recycling of catalysts from the liquid product solution becomes more readily after complete conversion of cellulose.

References

1   P. S. Shuttleworth, M. Debruyn, H. L. Parker, A. J. Hunt, V. L. Budarin, A. Matharu, J. Clark, *Green Chem.* 2014, **16**, 573-584.
2   M. Poliakoff, P. Licence, *Nature* 2007, **450**, 810-812.
3   Y. B. Huang, Y. Fu, *Green Chem.* 2013, **15**, 1095-1111.
4   L. Liu, L. Lin, Z. Wu, S. Y. Zhou, S. J. Liu, *Appl. Catal. B* 2015, **174-175**, 225-243.
5   W. S. Mok, M. J. Antal Jr, G. Varhegyi, *Ind. Eng. Chem. Res.* 1992, **31**, 94-100.
6   L. Kupiainen, J. Ahola, J. Tanskanen, *Ind. Eng. Chem. Res.* 2012, **51**, 3295-3300.
7   R. Rinaldi, N. Meine, J. vom Stein, R. Palkovits, F. Schüth, *ChemSusChem* 2010, **3**, 266-276.
8   A. A. Rosatella, S. P. Simeonov, R. F. M. Frade, C. A. M. Afonso, *Green Chem.* 2011, **13**, 754-793.
9   C. Tagusagawa, A. Takagaki, A. Iguchi, K. Takanabe, J. N. Kondo, K. Ebitani, T. Tatsumi, K. Domen, *Chem. Mater.* 2010, **22**, 3072-3078.
10 C. Tagusagawa, A. Takagaki, A. Iguchi, K. Takanabe, J. N. Kondo, K. Ebitani, S. Hayashi, T. Tatsumi, K. Domen, *Angew. Chem., Int. Ed.* 2010, **49**, 1128-1132.
11 J. Xi, Y. Zhang, Q. Xia, X. Liu, J. Ren, G. Lu, Y. Wang, *Appl. Catal. A* 2013, **459**, 52-58.
12 P. Sun, X. Long, H. He, C. Xia, F. Li, *ChemSusChem* 2013, **6**, 2190-2197.
13 A. A. Dwiatmoko, J. W. Choi, D. J. Suh, Y. Suh, H. H. Kung, *Appl. Catal. A* 2010, **387**, 209-214.
14 X. Qi, M. Watanabe, T. M. Aida, R. L. Smith Jr, *Green Chem.* 2008, **10**, 799-805.
15 K. Fukuhara, K. Nakajima, M. Kitano, H. Kato, S. Hayashi, M. Hara, *ChemSusChem* 2011, **4**, 778-784.
16 F. Tao, H. Song, L. Chou, *Bioresour Technol.* 2011, **102**, 9000-9006.
17 Y. Ogasawara, S. Itagaki, K. Yamaguchi, N. Mizuno, *ChemSusChem* 2011, **4**, 519-525.
18 D. Lai, L. Deng, Q. Guo, Y. Fu, *Energy Environ. Sci.* 2011, **4**, 3552-3557.
19 D. Lai, L. Deng, J. Li, B. Liao, Q. Guo, Y. Fu, *ChemSusChem* 2011, **4**, 55-58.
20 H. Cai, C. Li, A. Wang, G. Xu, T. Zhang, *Appl. Catal. B* 2012, **123–124**, 333-338.
21 J. A. Geboers, S. V. Vyver, R. Ooms, B. O. Beeck, P. A. Jacobs, B. F. Sels, *Catal. Sci. Technol.* 2011, **1**, 714-726.
22 Z. Shan, H. Wan, X. Meng, S. Liu, L. Wang, C. Wang, *Chem. Commun.* 2011, **47**, 1048-1050.
23 X. B. Ke, X. G. Zhang, H. W. Liu, S. Xue, H. Y. Zhu, *Chem. Commun.* 2013, **49**, 9866-9868.
24 S. Linic, U. Aslam, C. Boerigter, M. Morabito, *Nature. Mater.* 2015, **14**, 567-576.

25 A. Marimuthu, J. W. Zhang, S. Linic, *Science* 2013, **339**, 1590-1593.
26 X. G. Zhang, X. B. Ke, A. J. Du, H. Y. Zhu, *Sci. Rep.* 2014, **4**, 3805.
27 X. G. Zhang, A. J. Du, H. Y. Zhu, J. Jia, J. Wang, X. B. Ke, *Chem. Commun.* 2014, **50**, 1389-1391.
28 Z. Zhang, I. O'Hara, W. Doherty, G*reen Chem.* 2013, **15**, 431-438.
29 S. Yu, H. M. Brown, X. Huang, X. D. Zhou, J. E. Amonette, Z. C. Zhang, *Appl. Catal. A* 2009, **361**, 117-122.
30 H. B. Zhao, J. E. Holladay, H. M. Brown, Z. C. Zhang, *Science* 2007, **316**, 1597-1600.
31 B. Girisuta, L. P. B. M. Janssen, H. J. Heeres, *Ind. Eng. Chem. Res.* 2007, **46**, 1696-1708.
32 S. I. Naya, A. Inoue, H. Tada, *ChemPhysChem*. 2011, **12**, 2719-2723.
33 G. Baffou, R. Quidant, *Chem. Soc. Rev*. 2014, **43**, 3898-3907.
34 T. T. Jiang, C. C. Jia, L. C. Zhang, S. R. He, Y. H. Sang, H. D. Li, Y. Q. Li, X. H. Xu, H. Liu, *Nanoscale* 2015, **7**, 209-217.

Journal Name

COMMUNICATION

Table of Contents Graphic and Synopsis

Sustainable conversion of cellulosic biomass to chemicals under visible-light irradiation

Lina Wang,[a] Zhanying Zhang,[b] Lixiong Zhang,[c] Song Xue,[d] William O. S. Doherty,[b] Ian M. O'Hara [b] and Xuebin Ke*[a]

Plasmonic nanostructure: a high conversion (> 60%) of crystalline cellulose to chemicals was achieved with enhanced electromagnetic fields, $E/E_0 = 10^3$-10^6 times.